



HAL
open science

A selection of theoretical results in the context of laser-plasma interaction and inertial fusion

Patrick Mora

► **To cite this version:**

Patrick Mora. A selection of theoretical results in the context of laser-plasma interaction and inertial fusion. *High Energy Density Physics*, 2020, 34, pp.100744 -. 10.1016/j.hedp.2020.100744 . hal-03490000

HAL Id: hal-03490000

<https://hal.science/hal-03490000>

Submitted on 21 Jul 2022

HAL is a multi-disciplinary open access archive for the deposit and dissemination of scientific research documents, whether they are published or not. The documents may come from teaching and research institutions in France or abroad, or from public or private research centers.

L'archive ouverte pluridisciplinaire **HAL**, est destinée au dépôt et à la diffusion de documents scientifiques de niveau recherche, publiés ou non, émanant des établissements d'enseignement et de recherche français ou étrangers, des laboratoires publics ou privés.



Distributed under a Creative Commons Attribution - NonCommercial 4.0 International License

A selection of theoretical results in the context of laser-plasma interaction and inertial fusion

Patrick Mora

CPHT, CNRS, Ecole Polytechnique, Institut Polytechnique de Paris, 91128 Palaiseau, France

Abstract

I recall a selection of my results of the last 40 years. I first present a theoretical model of absorption of laser light by a plasma, with an emphasis on its dependence on the laser intensity and wavelength. A second topic concerns the nonlinear and nonlocal electron transport in steep temperature gradients. Thirdly, I present the work on the propagation of a short intense laser pulse in tenuous plasmas. Finally, I discuss the plasma expansion into a vacuum, in particular the structure of the ion front and the prediction of the maximum velocity attained by the ions in the expansion.

Keywords: laser-plasma interaction, inertial fusion, collisional absorption, thermal conduction, plasma expansion

1. Introduction

In this Teller lecture I recall a selection of my results of the last 40 years. One of my first work was a theoretical model of absorption of laser light by a plasma. This model coupled the absorption itself, the energy transport, and the hydrodynamics [1]. The idea
5 was to understand the dependence of the laser light absorption on the laser intensity and wavelength. Secondly, an important problem in the early years of inertial confinement fusion was the electron thermal transport in steep temperature gradients. With J.-F. Luciani, we proposed in 1983 a nonlinear and nonlocal theory of electron transport which helped to interpret experimental results showing a strong departure of the electron transport with
10 respect to the linear law of Spitzer and Härm [2]. Thirdly, with the outbreak of ultra-short laser pulses and the concept of fast ignition, the question of the propagation of a short laser pulse in tenuous plasmas arose. In 1992, with T.M. Antonsen, we elaborated a model, exhibiting its self focusing character and its tendency to develop Raman-like instabilities [3, 4]. We developed a laser plasma simulation code (WAKE) [5] which is much quicker than
15 usual particle-in-cell codes when applied to numerous experimental situations. In particular, this code enabled the first simulation of the complete cavitation of the electron density in the so-called bubble regime, which plays a crucial role in the obtainment of high energy

Email address: patrick.mora@polytechnique.edu (Patrick Mora)

Preprint submitted to High Energy Density Physics

January 7, 2020

quasi-monoenergetic electrons by laser-plasma acceleration [6]. Finally I worked on plasma expansion into a vacuum, in order to give a complete understanding of the structure of the flow, to elucidate the structure of the ion front, and to predict the maximum velocity attained by the ions in the expansion [7].

2. A theoretical model of absorption of laser light by a plasma

In the first decade of the studies on inertial confinement fusion, there has been a considerable interest in experiments using short-wavelength radiation as a possible fusion driver because of increased absorption and ablation pressure [8]. In a simple model [1], I tried to describe the behavior of quantities such as the absorption rate or the ablation pressure as functions of the parameters of the experiments, such as the light intensity I and the laser wavelength λ . In this lecture I briefly present the simplest version of this model. A more detailed discussion can be found in Ref. [1].

The model is based on the following hypotheses.

- (1) The laser energy is absorbed by inverse bremsstrahlung.
- (2) The electron density profile is described by an exponential function,

$$n_e = n_c \exp\left(\frac{x}{L}\right), \quad (1)$$

where n_c is the critical density associated with the laser wavelength λ , $n_c \propto \lambda^{-2}$, and where L is the density scalelength.

- (3) The dependence of the Coulomb logarithm on the plasma density and temperature is neglected, so that one has $\nu_c \propto n_c/T^{3/2}$, where ν_c is the collision frequency at the critical density and T is the electron temperature at the critical density.
- (4) The temperature is uniform in the underdense density profile, so that the collision frequency ν is proportional to the electron density, $\nu = (n_e/n_c)\nu_c$, and the absorption rate A is then given by [9]

$$A = 1 - \exp\left(-\frac{8}{3} \frac{\nu_c L}{c}\right). \quad (2)$$

- (5) The density scalelength L is supposed to be equal to the product $c_s \tau$, where $c_s \propto T^{1/2}$ is the ion acoustic velocity at the critical density and τ the pulse duration.
- (6) The electron temperature T is estimated by equating the absorbed energy flux AI to the energy necessary to maintain a self-similar isothermal expansion from the critical density to the vacuum,

$$AI = 4n_c T c_s. \quad (3)$$

Focusing on the wavelength dependence, one deduces from the first five hypotheses the following scaling law,

$$T \propto \frac{1}{\lambda^2 \ln[1/(1-A)]}. \quad (4)$$

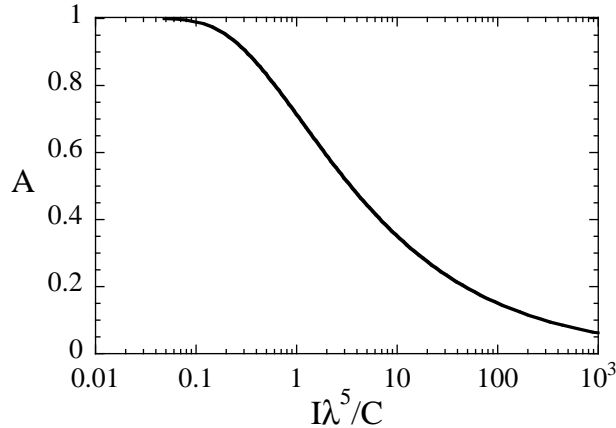


Figure 1: Absorption rate A as a function of $I\lambda^5$.

On the other hand the last hypothesis implies

$$AI \propto T^{3/2}/\lambda^2. \quad (5)$$

Eliminating the temperature T between these two equations results in

$$I\lambda^5 \propto \frac{1}{A\{\ln[1/(1-A)]\}^{3/2}}, \quad (6)$$

50 that is

$$A = 1 - \exp \left[- \left(\frac{C}{AI\lambda^5} \right)^{2/3} \right], \quad (7)$$

where C is a physical quantity which depends on the material and on the pulse duration [1]. The absorption rate A is represented in Fig. 1 as a function of the product $I\lambda^5$. An important feature of the model is that it shows the strong dependence of the absorption rate on the laser wavelength.

55 In the high intensity limit ($A \ll 1$) one easily finds the scaling law $P_a \propto I^{2/5}\lambda^{-2}$, where P_a is the ablation pressure. However, in this limit, it must be pointed out that other absorption mechanisms may become important, such as resonance absorption at the critical density [12].

To treat the low intensity limit, $(1 - A) \ll 1$, it is necessary to reconsider the model, since the laser energy is in fact totally absorbed before reaching the critical density. If n_0 60 denotes the electron density actually attained by the laser light, Eq. (3) should be replaced by $I = 4n_0 T c_s$ (here T is the temperature in the part of the density profile below n_0). The density n_0 is evaluated by assuming that the optical thickness from the vacuum to the point of density n_0 is of order 1. This is the self-regulating rarefaction as described for instance in Ref. [10]. The following new scaling law, $P_a \propto I^{3/4}\lambda^{-1/4}$, is then obtained. This regime is 65 of particular interest in the context of material processing [11].

The model can be easily adapted to the case where the length L is limited, for instance by the geometry of the laser-target interaction. In this case the relevant parameter becomes

the product $I\lambda^4$ which still exhibits a strong dependence on the laser wavelength. New scaling laws can be deduced in this regime, leading to $P_a \propto I^{1/3}\lambda^{-2}$ in the high intensity limit and $P_a \propto I^{7/9}\lambda^{-2/9}$ in the low intensity limit.

3. Electron transport in steep temperature gradients

The second work described in this lecture concerns electron thermal transport in steep temperature gradients. Experimental results in the context of laser-plasma interaction and kinetic Fokker-Planck simulations [13] have shown that the electron heat flux predicted by the Spitzer-Härm theory [14],

$$\mathbf{q}_{SH} = -\kappa \nabla T, \quad (8)$$

usually overestimates the actual heat flux in the case of strong temperature gradients (see Fig. 2 for a typical result). The absolute value of the heat flux seems to be limited to a fraction $f \approx 0.1 - 0.2$ of the free-streaming value

$$q_{FS} = n_e m_e v_e^3, \quad (9)$$

where $v_e = (k_B T / m_e)^{1/2}$ is the electron thermal velocity. On the other hand, a few tens of thermal electron mean free paths away from the heat front, the conductivity exceeds the Spitzer-Härm conductivity because the flux has a nonlocal part due to the hot, nearly collisionless electrons streaming away from the top of the heat front. In 1983, extending an idea formulated in the context of electron energy transport in ion waves [15], we proposed a nonlocal one-dimensional expression for the heat flux [2, 16],

$$q_e(x) = \int q_{SH}(x') w(x, x') dx', \quad (10)$$

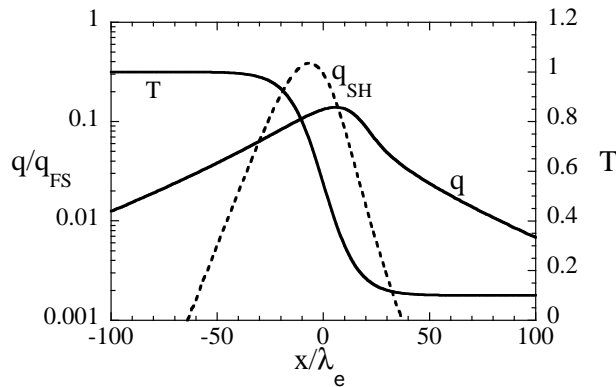


Figure 2: Typical result of a Fokker-Planck simulation for a temperature profile with a steep gradient. The temperature T is normalized to the temperature on the hot (left) side. q_{SH} is the heat flux predicted by the Spitzer-Härm theory and q is the actual heat flux. Both quantities are normalized to the free-streaming value q_{FS} calculated on the hot side. The position x is normalized to the thermal electron mean free path λ_e determined on the hot side.

85 where the kernel $w(x, x')$ is given by

$$w(x, x') = \frac{1}{2\lambda(x')} \exp \left[-\frac{X}{\lambda(x')} \right], \quad (11)$$

with

$$X = \frac{1}{n_e(x')} \left| \int_x^{x'} n_e(x'') dx'' \right|, \quad (12)$$

and where $\lambda(x')$ is the effective range of the electrons coming from the part of the profile corresponding to a temperature $T(x')$, and that carry the heat flux,

$$\lambda(x') \simeq 30\sqrt{Z+1} \lambda_e(x'), \quad (13)$$

where $\lambda_e(x')$ denotes the mean free path of thermal electrons corresponding to the temper-
 90 ature $T(x')$. In this expression, the factor $\sqrt{Z+1}$ comes from the fact that the electrons have to be slowed down by electron-electron collisions while they are deflected mainly by electron-ion collisions.

The nonlocal expression (10) fits quite accurately the heat flow predicted by Fokker-Planck simulations. It coincides with the Spitzer-Härm expression for gentle temperature
 95 and density gradients, for which $w(x, x')$ behaves as a δ -function of $x' - x$. On the other hand, for very steep temperature gradients, it predicts a maximum heat flux on the order of $0.1 - 0.2 q_{FS}$, the numerical factor depending on Z . Finally it exhibits the nonlocal character due to the hot, nearly collisionless, electrons streaming away from the hot part of the plasma.

100 Analytical justifications of the nonlocal formula (10) were established in the '80. Various delocalization propagators have also been proposed by different authors. A review and more references are given in [16]. Such nonlocal formulas have been introduced in fluid codes to model heat transport. One of the most recent model is the one by Schurtz et al. [17] which extends formula (10) to two or three dimensions of space. Such models are essential in the
 105 physics of targets of inertial fusion [18, 19].

4. Propagation of a short laser pulse in tenuous plasmas

The technique of chirped pulse amplification (CPA) for amplifying an ultrashort laser pulse was introduced by D. Strickland and G. Mourou in 1985 [20]. With the outbreak of
 110 ultrashort intense laser pulses, various applications were proposed, such as the fast ignition of thermonuclear targets [21] or the acceleration of electrons to high energies [22, 23, 24]. In these contexts, the question of the propagation of short laser pulses in tenuous plasmas arose. While particle-in-cell simulations are relevant for studying such a question, they are time-consuming and do not allow to scan a large range of parameters. On the other hand, a ponderomotive approach is made possible when two conditions are fulfilled [5], (i)
 115 the laser frequency ω_0 is much larger than the electron plasma frequency ω_p , and (ii) the quasistatic approximation is valid, i.e., the electron transit time through the laser pulse is

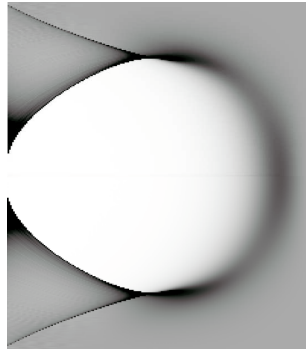


Figure 3: Bubble regime. The electron density is represented in gray scale (saturated to 2.5 times initial density). The laser pulse corresponds to the following parameters, $a_{max}^2 = 12.5$, $\omega_p \tau_0 = 6/\pi$, and $k_p w_0 = 2.5$. The longitudinal axis corresponds to the range $k_p z - \omega_p t = [-7, +3]$, and the transverse axis to $k_p r = [-5.5, +5.5]$.

short compared with the characteristic laser pulse deformation time (this approximation is valid for plasma electrons of sufficiently low energy).

The laser radiation is described in terms of the high-frequency vector potential \mathbf{A}_\perp , which can be written in the form of an envelope $\hat{\mathbf{A}}_\perp$ modulating a plane wave traveling at the speed of light. The envelope depends on time and space and is determined by

$$\left[\frac{2}{c} \frac{\partial}{\partial t} \left(ik_0 + \frac{\partial}{\partial \zeta} \right) + \nabla_\perp^2 \right] \hat{\mathbf{A}}_\perp = \frac{e^2}{m \epsilon_0 c^2} \left\langle \frac{\bar{n}}{\bar{\gamma}} \right\rangle \hat{\mathbf{A}}_\perp, \quad (14)$$

where $k_0 \approx \omega_0/c$ is the wave number of the plane wave and $\zeta = z - ct$ measures the distance back from the head of the pulse. The right-hand side of Eq. (14) represents the dielectric response of the plasma. The angular bracket represents an ensemble average over a distribution of particles, each member of which has a density, \bar{n} , and a relativistic factor, $\bar{\gamma}$, where the overbar on each quantity signifies that it is slowly varying in time.

The motion of the particles is due to the combined effect of the electromagnetic fields of the wake and of the ponderomotive potential of the laser pulse,

$$\frac{d\bar{\mathbf{p}}}{dt} = -e (\bar{\mathbf{E}} + \bar{\mathbf{v}} \times \bar{\mathbf{B}}) - \frac{e^2}{2\bar{\gamma}m} \nabla \bar{A}_\perp^2, \quad (15)$$

while the average relativistic factor is given by

$$\bar{\gamma} = \sqrt{1 + \frac{1}{m^2 c^2} (\bar{p}^2 + e^2 \bar{A}_\perp^2)}. \quad (16)$$

We have solved the set of Eqs. (14-16) and the equations for the fields of the wake on two-dimensional Cartesian or cylindrical grid with the computer code WAKE [5]. Such a code can be useful to describe laser self-focusing and Raman-type instabilities [3, 4, 6].

Here we show an example of simulation in a case corresponding to the so-called cavitation or bubble regime [6, 25, 26, 27, 28]. To simplify the presentation, we introduce the following

135 normalized vector potential: $\mathbf{a} = e\mathbf{A}_\perp/mc$. We also define the time $\tau = \zeta/c$ and the plasma wavevector $k_p = \omega_p/c$, where ω_p is the plasma frequency. Figure 3 shows the electron density in the wake of a laser pulse of the form

$$a^2(\tau, \mathbf{r}_\perp) = a_{max}^2 \exp\left(-2r_\perp^2/w_0^2\right) \cos^2(\tau/\tau_0), \quad (17)$$

with $|\tau| < (\pi/2)\tau_0$ (the pulse is limited to one arch), with the following parameters, $a_{max}^2 = 12.5$, $\omega_p\tau_0 = 6/\pi$, and $k_pw_0 = 2.5$. The laser pulse (not shown) has its front on the right side of the figure. One observes the total electron cavitation in the wake and a transverse wavebreaking responsible of the two black lines escaping from the bubble. It is important to point out that, though the code enables the identification of the cavitation regime, it does not have the capacity of exhibiting the longitudinal electron acceleration and trapping at the back of the bubble [25], where the quasistatic approximation becomes invalid for those
145 electrons.

5. Plasma expansion into a vacuum

Ultrashort and ultraintense laser pulses can also be used to accelerate ions to high energy. Experiments about 20 years ago produced such high-energy ion jets from the interaction of short laser pulse with solid targets (see [29] and [30] for a list of references). Though widely
150 used in the interpretation of the experimental results [31], at this time the freely expanding plasma model [32, 33, 34] has not been fully explored in terms of charge separation effects and structure of the ion front. The objective of this last work was to fill this gap [7].

Let us first recall the fundamentals of the model. At time $t=0$, a plasma is assumed to occupy the half-space $x < 0$. The ions are cold and initially at rest with density $n_i = n_{i0}$
155 for $x < 0$ and $n_i = 0$ for $x > 0$ with a sharp boundary, while the electron density n_e is continuous and corresponds to a Boltzmann distribution,

$$n_e = n_{e0} \exp(e\Phi/k_B T), \quad (18)$$

where n_{e0} is the electron density in the unperturbed plasma (i.e., for $x = -\infty$), Φ is the electrostatic potential, and T is the electron temperature, which may be in the relativistic domain. The potential Φ satisfies the Poisson equation,

$$\epsilon_0 \partial^2 \Phi / \partial x^2 = e(n_e - Zn_i), \quad (19)$$

160 where Z is the ion charge number. At $x = -\infty$ one has $\Phi = 0$ and $n_{e0} = Zn_{i0}$.

For $t > 0$ the electrons are assumed to stay in equilibrium with the potential Φ , so that Eqs. (18) and (19) still hold, while the ion expansion into a vacuum is described by the equations of continuity and motion

$$(\partial/\partial t + v_i \partial/\partial x) n_i = -n_i \partial v_i / \partial x, \quad (20)$$

$$(\partial/\partial t + v_i \partial/\partial x) v_i = -(Ze/m_i) \partial \Phi / \partial x, \quad (21)$$

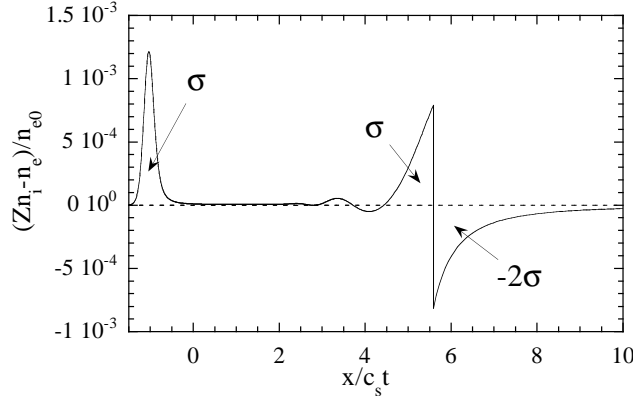


Figure 4: Charge separation at time $\omega_{pi}t = 50$. The ion front stands at $x/c_s t \simeq 5.59$.

165 where v_i is the ion velocity. For $x + c_s t > 0$, a self-similar expansion is found if one assumes quasineutrality in the expanding plasma, with $n_e = Zn_i = n_{e0} \exp(-x/c_s t - 1)$, $v_i = c_s + x/t$, and

$$E_{ss} = k_B T / e c_s t = E_0 / \omega_{pi} t, \quad (22)$$

where ss stands for self-similar, $c_s = (Zk_B T / m_i)^{1/2}$ is the ion acoustic velocity, $E_0 = (n_{e0} k_B T / \epsilon_0)^{1/2}$, and $\omega_{pi} = (n_{e0} Z e^2 / m_i \epsilon_0)^{1/2}$ is the ion plasma frequency. The self-similar 170 field corresponds to a positive charge surface $\sigma = \epsilon_0 E_{ss}$ per unit surface at position $x = -c_s t$, and a negative charge surface $-\sigma$ at the plasma edge.

First, the self-similar solution has no meaning as long as the initial Debye length, $\lambda_{D0} = (\epsilon_0 k_B T / n_{e0} e^2)^{1/2}$, is larger than the self-similar density scale length, $c_s t$, i.e., for $\omega_{pi} t < 1$. Secondly, for $\omega_{pi} t \gg 1$, the self-similar model predicts a velocity increasing without limit 175 for x going to infinity. Physically the ion velocity is limited to a finite value and the ions originally at $x = 0$ form a well-defined ion front [33].

To clear up these issues, I have developed a Lagrangian code that takes into account the charge separation effects and thus solves Eqs. (18), (19), (20) and (21). The numerical methods are similar to that described in [35]. As an example of the results of the code, 180 Fig. 4 shows the charge separation as a function of space at time $\omega_{pi} t = 50$, for which the ion front stands at $x/c_s t \simeq 5.59$. Three distinct nonneutral zones are clearly seen: a first positive layer of total charge $\sigma = \epsilon_0 E_{ss}$ per unit surface around the position $x = -c_s t$, where the expansion starts, a second positive layer of same total charge σ just on the left of the ion front, and a negative layer due to the electron cloud on its right, with charge -2σ . As 185 expected, the total charge around the ion front is $-\sigma$.

The corresponding electric field is shown in Fig. 5 at the same time, showing the rapid increase of the electric field in the vicinity of the ion front. Such a peak has been experimentally observed in [36]. A precise analytical fit for the electric field at the ion front, valid for any time, is

$$E_{front} \simeq 2E_0 / (2e + \omega_{pi}^2 t^2)^{1/2}. \quad (23)$$

190 Accurate predictions can be made for the characteristics of the ion front. Integrating

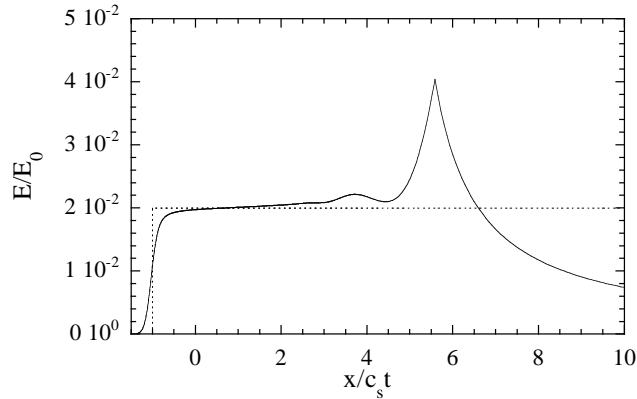


Figure 5: Electric field at time $\omega_{pi}t = 50$. The ion front stands at $x/c_s t \simeq 5.59$ where the electric field peaks. The dotted line corresponds to the usual self-similar solution, Eq. (22). Note that the electric field at the ion front is approximately twice the self-similar field as predicted by Eq. (23).

$dv_{front}/dt = ZeE_{front}/m_i$ and $dx_{front}/dt = v_{front}$, one obtains successively the ion front velocity and position as functions of time,

$$v_{front} \simeq 2c_s \ln \left(\tau + \sqrt{\tau^2 + 1} \right), \quad (24)$$

$$x_{front} \simeq 2\sqrt{2e}\lambda_{D0} \left[\tau \ln \left(\tau + \sqrt{\tau^2 + 1} \right) - \sqrt{\tau^2 + 1} + 1 \right], \quad (25)$$

where $\tau = \omega_{pi}t/\sqrt{2e}$.

195 The preceding results apply for a semi-infinite plasma. Finite size effects manifest themselves in a further limitation of the maximum ion energy due to electron cooling during the plasma expansion [37, 38].

6. Conclusion

200 I reviewed some of my results obtained over the last 40 years on the physics of laser-plasma interaction and applications. The main common feature of these works is that they always tried to give a picture of plasma effects, using simple tools, as opposed to many theoretical works based upon large size computer codes.

References

- 205 [1] P. Mora, Theoretical model of absorption of laser light by a plasma, Phys. Fluids 25 (1982) 1051–1056.
 [2] J. F. Luciani, P. Mora, J. Virmont, Non local heat transport due to steep temperature gradient, Phys. Rev. Lett. 51 (1983) 1664–1667.
 [3] T. M. Antonsen, Jr., P. Mora, Self-focusing and Raman scattering of laser pulses in tenuous plasmas, Phys. Rev. Lett. 69 (15) (1992) 2204–2207.
 210 [4] T. M. Antonsen, Jr., P. Mora, Self-focusing and Raman scattering of laser pulses in tenuous plasmas, Phys. Fluids B 5 (5) (1993) 1440.

- [5] P. Mora, T. M. Antonsen, Jr., Kinetic modeling of intense, short laser pulses propagating in tenuous plasmas, *Phys. Plasmas* 4 (1) (1997) 217–229.
- [6] P. Mora, T. M. Antonsen, Jr., Electron cavitation and acceleration in the wake of an ultra-intense, self-focused laser pulse, *Phys. Rev. E* 53 (3) (1996) R2068–R2071.
- 215 [7] P. Mora, Plasma expansion into a vacuum, *Phys. Rev. Lett.* 90 (2003) 185002.
- [8] C. Garban-Labaune, E. Fabre, C. Max, R. Fabbro, F. Amiranoff, J. Virmont, M. Weinfeld, A. Michard, Effect of laser wavelength and pulse duration on laser light absorption and backreflection, *Phys. Rev. Lett.* 48 (1982) 1018–1021.
- [9] W. L. Kruer, *The physics of laser plasma interactions*, Addison-Wesley, New-York, 1988.
- 220 [10] A. Caruso, R. Gratton, Some properties of the plasmas produced by irradiating light solids by laser pulses, *Plasma Phys.* 10 (1968) 867.
- [11] C. Momma, B. N. Chichkov, S. Nolte, F. von Alvensleben, A. Tunnermann, H. Welling, B. Welleghausen, Short-pulse laser ablation of solid targets, *Opt. Commun.* 129 (1996) 134.
- [12] V. L. Ginzburg, *The properties of electromagnetic waves in plasmas*, Pergamon, New York, 1964.
- 225 [13] A. R. Bell, R. G. Evans, D. J. Nicholas, Electron energy transport in steep temperature gradients in laser-produced plasmas, *Phys. Rev. Lett.* 46 (1981) 243.
- [14] L. Spitzer, R. Härm, Transport phenomena in a completely ionized gas, *Phys. Rev.* 89 (1953) 977.
- [15] A. R. Bell, Electron energy transport in ion waves and its relevance to laser-produced plasmas, *Phys. Fluids* 26 (1983) 279.
- 230 [16] P. Mora, J. F. Luciani, Non local electron transport in laser created plasmas, *Laser and Particle Beams* 12 (1994) 387.
- [17] G. P. Schurtz, P. D. Nicolai, M. Busquet, A nonlocal electron conduction model for multidimensional radiation hydrodynamics codes, *Phys. Plasmas* 7 (2000) 4238.
- [18] S. Atzeni, J. Meyer-ter-Vehn, *The physics of inertial fusion*, Clarendon Press, Oxford, 2004.
- 235 [19] J. D. Lindl, P. Amendt, R. L. Berger, S. Glendinning, S. H. Glenzer, S. W. Haan, R. L. Kauffman, O. L. Landen, L. J. Suter, Ion acceleration by superintense laser-plasma interaction, *Phys. Plasmas* 11 (2004) 339.
- [20] D. Strickland, G. Mourou, Compression of amplified chirped optical pulses, *Opt. Commun.* 56 (1985) 219.
- 240 [21] M. Tabak, J. Hammer, M. E. Glinsky, W. L. Kruer, S. C. Wiks, J. Woodworth, E. M. Campbell, M. D. Perry, R. J. Mason, Ignition and high gain with ultrapowerful lasers, *Phys. Plasmas* 1 (5) (1994) 1626–1634.
- [22] L. M. Gorbunov, V. I. Kirsanov, Excitation of plasma waves by an electromagnetic wave packet, *Sov. Phys. JETP* 66 (1987) 290.
- 245 [23] F. Amiranoff, S. Baton, D. Bernard, B. Cros, D. Deschamps, F. Dorchies, F. Jacquet, V. Malka, J.-R. Marquès, G. Matthieussent, P. Min, A. Modena, P. Mora, J. Morillo, Z. Najmudin, Observation of laser wakefield acceleration of electrons, *Phys. Rev. Lett.* 81 (1998) 995.
- [24] E. Esarey, C. B. Schoeder, W. P. Leemans, Physics of laser-driven plasma-based electron accelerators, *Rev. Mod. Phys.* 81 (2009) 1229.
- 250 [25] A. Pukhov, J. Meyer-ter-Vehn, Laser wake field acceleration: the highly non-linear broken-wave regime, *Appl. Phys. B: Lasers Opt.* 74 (2002) 355.
- [26] J. Faure, Y. Glinec, A. Pukhov, S. Kiselev, S. Gordienko, E. Lefebvre, J.-P. Rousseau, F. Burgy, V. Malka, A laser-plasma accelerator producing monoenergetic electron beams, *Nature* 431 (2004) 541.
- 255 [27] S. P. D. Mangles, C. D. Murphy, Z. Najmudin, A. G. Thomas, J. L. Collier, A. E. Dangor, E. J. Divall, P. S. Foster, J. G. Gallacher, C. J. Hooker, D. A. Jaroszynski, A. J. Langley, W. B. Mori, P. A. Norreys, F. S. Tsung, R. Viskup, B. R. Walton, K. Krushelnick, Monoenergetic beams of relativistic electrons from intense laser-plasma interactions, *Nature* 431 (2004) 535.
- [28] C. G. R. Geddes, C. Toth, J. van Tilborg, E. Esarey, C. B. Schroeder, D. Bruhwiler, C. Nieter, J. Cary, W. P. Leemans, High-quality electron beams from a laser wakefield accelerator using plasma-channel guiding, *Nature* 431 (2004) 538.
- 260 [29] J. Fuchs, P. Antici, E. D’Humieres, E. Lefebvre, M. Borghesi, E. Brambrink, C. Cecchetti, M. Kaluza,

V. Malka, M. Manclossi, S. Meyroneinc, P. Mora, J. Schreiber, T. Toncian, H. Pepin, P. Audebert, Laser-driven proton scaling laws and new paths towards energy increase, *Nature Phys.* 2 (2006) 48.

265 [30] A. Macchi, M. Borghesi, M. Passoni, Ion acceleration by superintense laser-plasma interaction, *Rev. Mod. Phys.* 85 (2013) 751.

[31] S. C. Wilks, A. B. Langdon, T. E. Cowan, M. Roth, M. Singh, S. Hatchett, M. H. Key, D. Pennington, A. MacKinnon, R. A. Snavely, Energetic proton generation in ultra-intense laser-solid interactions, *Phys. Plasmas* 8 (2001) 542.

270 [32] A. V. Gurevich, L. V. Pariiskaya, L. P. Pitaevskii, Self-similar motion of rarefied plasma, *Sov. Phys. JETP* 22 (1966) 449.

[33] J. E. Crow, P. L. Auer, J. E. Allen, The expansion of a plasma into a vacuum, *J. Plasma Physics* 14 (1975) 65.

[34] P. Mora, R. Pellat, Self-similar expansion of a plasma into a vacuum, *Phys. Fluids* 22 (1979) 2300.

275 [35] M. A. True, J. R. Albritton, E. A. Williams, Fast ion production by suprathermal electrons in laser fusion plasmas, *Phys. Fluids* 24 (1981) 1885.

[36] L. Romagnani, J. Fuchs, M. Borghesi, P. Antici, P. Audebert, F. Ceccherini, T. Cowan, T. G. an, S. Kar, A. Macchi, P. Mora, G. Pretzler, A. Schiavi, T. Toncian, O. Willi, Dynamics of electric fields driving laser acceleration of multi-mev protons, *Phys. Rev. Lett.* 95 (2005) 195001.

[37] P. Mora, Thin-foil expansion into a vacuum, *Phys. Rev. E* 72 (2005) 056401.

280 [38] P. Mora, Collisionless expansion of a gaussian plasma into a vacuum, *Phys. Plasmas* 12 (2005) 112102.